EOSC 453 Assignment 2

Volcanic Eruptions and Climate Change

E. Giroud-Proeschel - 123456789
P. Matlashewski - 45701109
M. Ormerod - 16265167

November 20, 2020

Contents

1 Introduction

Anthropogenic global warming is an identifier of climate change and a defining issue of our time. It is thought to be the main trigger of intensified, more frequent extreme weather events, sea-level rise with the potential to displace millions, and loss of large freshwater reservoirs. The question of why, and how, climate change operates, and what we can do to mitigate its effects during our lifetime, is an arduously nonlinear problem that climate scientists still battle with, both in the laboratory and in politics. Within this contention, we focus on how large local out-gassing events of volatils such as sulfur dioxide during volcanic eruptions have historically affected the Earth's climate. Here we chose to investigate the impact of volcanic perturbations on a simple radiative energy balance model. Throughout this paper we will only consider the effect of aerosols, and more specifically, SO2. This model is inspired by the work of Russian climatologist Mikhail I. Budyko, who discovered the ice-albedo feedback mechanism underlying climate change through his pioneering of studies on global climate using physical models of equilibrium (eq of what???) (Budyko 1969). We proceed as follows:

1. Build a graphical algorithm solving the radiative energy balance equations in a zonally-averaged Earth model, based on figure 1
2. Compute the present, steady-state energy balance of the Earth to investigate the effect of intra-zonal transfer by:
3. setting all transfer coefficients kij to zero
4. using the provided values of kij and comparing heat transfer magnitude and rates from our previous step
5. from (Robock 2000) from the 1982 El Chichón and Pinatubo eruption introduce a $\phi(t)$ function representing the spatially and temporally reducing effects of aerosol outgassing on the incoming radiation
6. Consider a nonlinear effect of temperature on albedo.
7. Using this new albedo parameterization as a proxy for the "ice-albedo" feedback, we look for solutions favourable to Snowball Earth conditions.
8. We then implement a Poisson sampling of eruptions to investigate a volcanic solution to Snowball Earth

1.1 Budyko Climate Model

The evolution of Earth's temperature will be investigated using a Budyko climate model (Budyko 1969). The earth is divided into 6 latitudinal zones, defined by the latitudes shown in table 1 and figure 1.

Zone	Lower Latitude	Upper Latitude
1	$90°S$	$60°S$
2	$60°S$	$30°S$
3	$30°S$	$0°$
4	$0°$	$30°N$
5	$30°S$	$60°N$
6	$60°S$	$90°N$

Table 1: Zone latitudes.

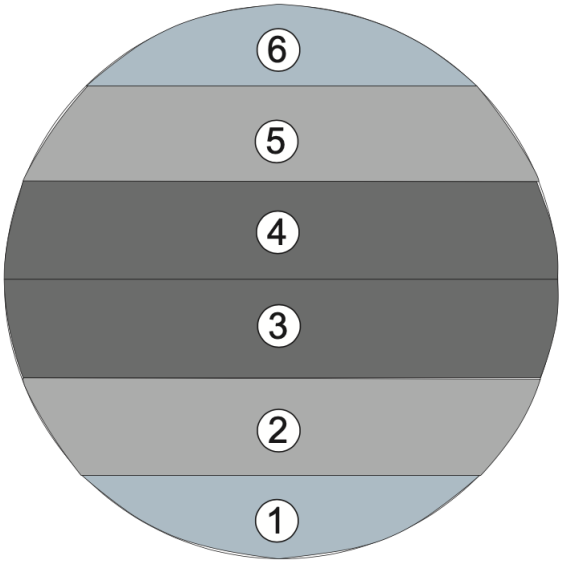

Figure 1: Latitude zone intervals.

Within each zone, temperature evolves through radiative heat fluxes entering the earth through solar radiation, heat fluxes leaving the earth as long-wave radiation and the exchange of heat between zones. These effects are quantified through

$$\frac{dT_k}{dt} = \frac{1}{\overline{\rho_k c_k[Z_k]}}\{\gamma_k(1-\alpha_k^{sky})(1-\bar{\alpha}_k)S_0 - \tau\sigma_B T_k^4\} + \frac{L_{ki}k_{ki}}{A_k\overline{\rho_k c_k[Z_k]}}(T_k - T_i) \tag{1}$$

where $k = 1, \ldots, 6$ represents each latitudinal zone and T_k is the zonal temperature. The remaining constants are defined in tables 9 and 10 of section 5.3.2.

1.2 Volcanic Eruptions

Volcanism is an important natural cause of climate change across a range of timescales (Robock 2000). For our investigation, we consider the short-term cooling effects of volcanism that occur on a $10-100$ year time frame. These cooling effects are introduced in our model by applying an occlusion factor, $\phi(t)$, to each zone in the model. The occlusion factor represents the presence of volcanic aerosols suspended in the atmosphere that block direct shortwave

solar radiation. The introduction of $\phi_k(t)$ transforms equation 1 to

$$\frac{dT_k}{dt} = \frac{1}{\rho_k c_k [Z_k]}\{\phi_k(t)\gamma_k(1-\alpha_k^{sky})(1-\bar{\alpha}_k)S_0 - \tau\sigma_B T_k^4\} + \frac{L_{ki}k_{ki}}{A_k\rho_k c_k [Z_k]}(T_k - T_i) \qquad (2)$$

A value of $\phi(t) = 1$ represents no volcanic aerosol occlusion. A value of $\phi(t) = 0.7$, for example, represents a 30% reduction in total incoming solar radiation.

1.2.1 Direct Radiation Occlusion

Based on observations of the reduction of solar radiation after the 1982 El Chichón eruption and the 1991 Pinatubo eruption (Robock 2000), an empirical curve for $\phi(t)$ was fit to the data, as shown in figure 2. We found that a function with the form $\phi(t) = 1 - ct^{-2}$, where $c = 5.36$ yr^2 is an empirical constant found through nonlinear regression, gave a reasonable representation of the data. Moreover, this function has the property that $\phi(t) \to 1$ as $t \to \infty$, which models the decaying effects of aerosol occlusion over time.

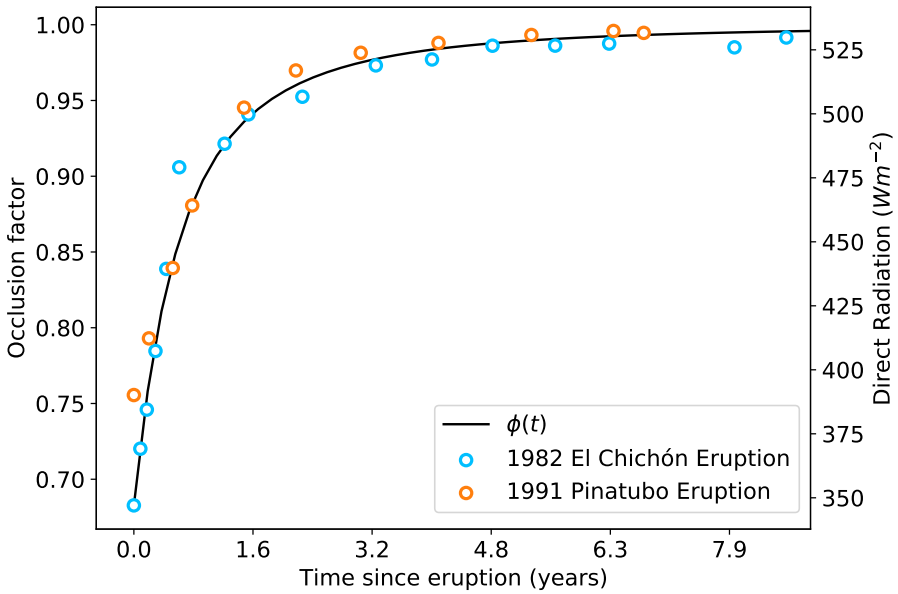

Figure 2: Plot of $\phi(t)$; occlusion factor. An occlusion factor of 0.7 represents a 30% reduction in total incoming solar radiation.

1.2.2 Spatial Distribution of Aerosols

The effects of a volcanic eruption are not local to a single zone. Suspended aerosols are dispersed throughout the atmosphere and can travel large distances across the Earth. To model the spatial effects of aerosol dispersion following an eruption, a time lag is introduced to the zonal occlusion functions, $\phi_k(t)$, that varies based on the distance zone k is from the eruption zone. An example is shown in figure 3, where an eruption occurs at $t = 0$ in zone 1. For the first 3 months following the eruption, only zone 1 has the occluding effects of volcanic aerosols. After 3 months, the aerosols have traveled to the adjacent zone 2, where $\phi_2(t)$ begins

to follow the decaying occlusion function defined in section 1.2.1. This process continues until the entire earth is affected by the volcanic aerosols after approximately 9 months. The specific lag times considered in the model were estimated from the data presented in Robock 2000.

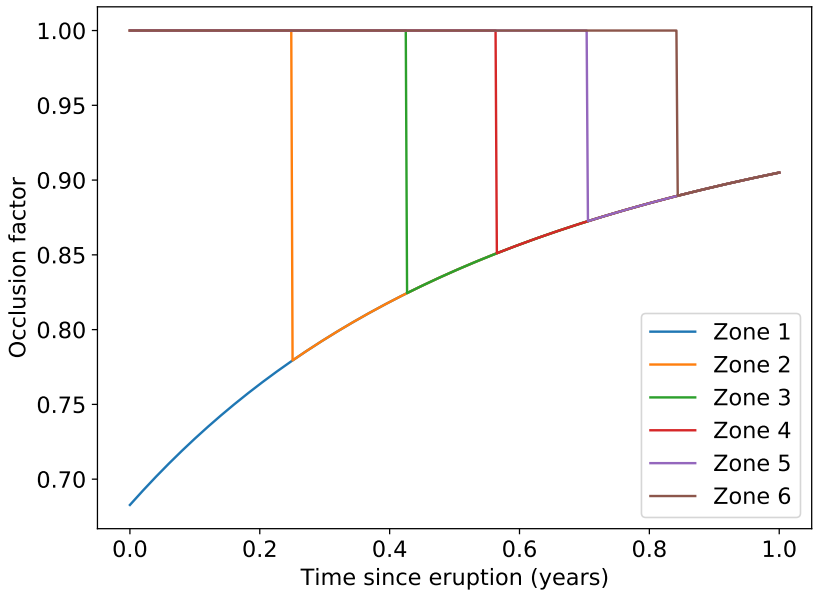

Figure 3: The spatial effect of eruptions. A distance-dependent time lag is present for zones adjacent to the eruption.

1.2.3 Stochastic Eruption Frequency

Sections 1.2.1 and 1.2.2 define our model's response to a single eruption. To investigate the intensity of volcanism on the Earth's climate, we allow for a series of eruptions to occur over time. Volcanic eruptions in each zone are modeled as a Poisson process, where each zone is prescribed an eruption frequency intensity, λ_k, that reflects the average repose time between eruptions in the zone. For an eruption intensity λ_k, the probability of a repose time, t_R, between eruptions follows an exponential distribution

$$P(t_R) = \lambda_k e^{-\lambda_k t_R} \tag{3}$$

For this investigation, we assume eruptions occur independently in each zone.

The intensity of volcanic activity on Earth can be adjusted by raising or lowering each zone's λ_k. A smaller λ_k represents shorter repose times and higher volcanic activity. Combining equation 3 with the occlusion function defined in sections 1.2.1 and 1.2.2 gives a simple stochastic model for volcanism on Earth that includes the time-decaying effects of aerosol occlusion, the spatial dispersion of aerosols and temporal volcanic intensity.

1.3 Ice-Albedo Feedback

The volcanism defined in section 1.2 provides a mechanism to cool the Earth by occluding direct solar radiation with suspended volcanic aerosols. One interesting way to study the implications of this cooling is by considering the ice-albedo feedback Budyko 1969. The idea of the ice-albedo feedback is that if the temperature of the Earth is cold enough, ice will grow and cover a larger proportion of the Earth's surface. This will result in a higher surface albedo, reflecting the incoming solar radiation. The higher albedo will further contribute to decreasing the temperature of the Earth, leading to a positive feedback. This runaway cooling has the potential to completely cover the Earth in ice, leading to a "Snowball Earth" scenario.

We model the ice-albedo feedback by defining a temperature dependent albedo as follows

$$\alpha_k(T_k) = \begin{cases} \alpha_{k0} & T_k \geq T_0 \\ \alpha_{k0} + (\alpha_i - \alpha_k)\frac{(T_k - T_0)^2}{(T_i - T_0)^2} & T_i < T_k < T_0 \\ \alpha_i & T_k \leq T_i \end{cases} \tag{4}$$

where α_k is the albedo in zone k, T_k is the temperature in zone k, $T_0 = 280$ K is the threshold temperature where we allow the growth of ice to increase the albedo, $T_i = 250$ K is the temperature where the zone is completely covered in ice, α_{k0} is the baseline zonal albedo given in table 9 and $\alpha_i = 0.6$ is the albedo of ice. Figure 4 shows the nonlinear albedo function for each zone.

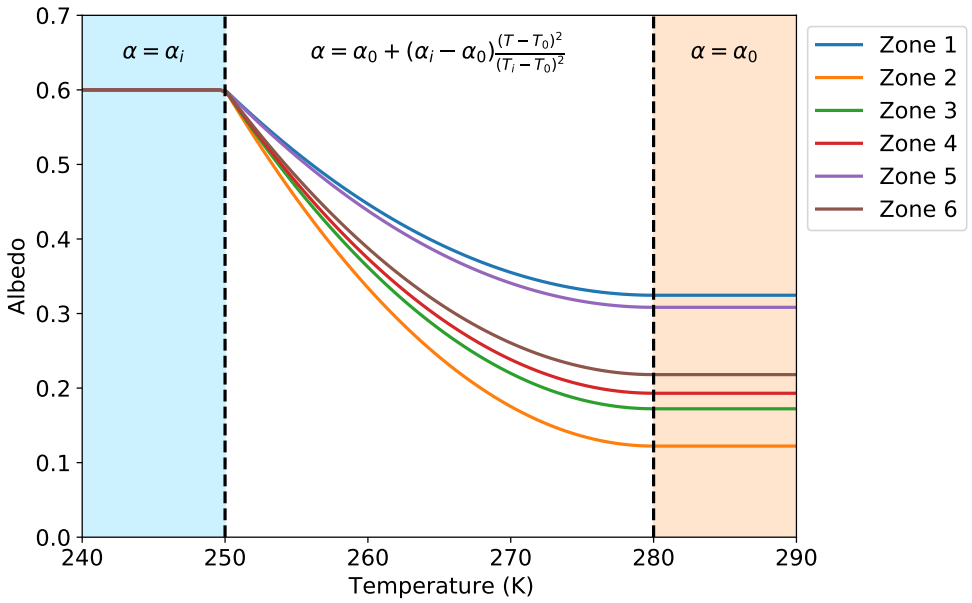

Figure 4: Albedo parameterization as a function of temperature in each zone. The blue shaded region indicates the temperature range where a zone is covered with ice. The orange shaded region indicates the temperature range where there is no change in ice as temperature varies.

Zone	Interzonal Transfer Supressed Equilibrium Temperature [K]	Interzonal Transfer Allowed Equilibrium Temperature [K]
1	217.23	274.12
2	279.74	279.34
3	296.45	282.26
4	294.56	280.88
5	263.56	279.71
6	225.33	274.93

Table 2: Equilibrium Temperature distributions for a climate model with no volcanism

2 Results

In this section, we will report on data obtained via our three forms of volcanic perturbations and describe the behaviours of these perturbations within the context of the data itself.

2.1 Steady-State Climate Model: No Volcanism

By passing initial condition temperatures calculated through our model with suppressed inter-zonal transfer (See Table 2) to our steady-state model where inter-zonal transfer is allowed, we solve for the equilibrium temperatures by integrating forward in time (Figure 5).

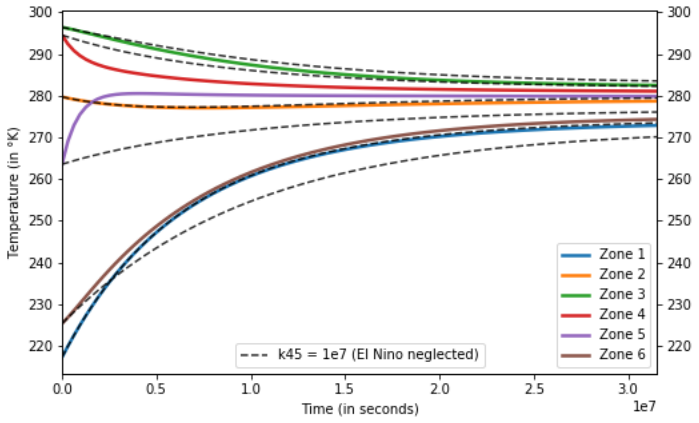

Figure 5: Equilibrium solution for 6-zoned Earth climate model. Zone 1 marks the southernmost band at $60 - 90°$S while zone 6 represents the northernmost band at $60 - 90°$N. Zones 2-5 are bands covering $30°$ intervals between zones 1 and 6 (See Figure 1).

There are a few key observations to note. The first is that a larger transfer coefficient (**??**), representing the northern Gulf Stream between zones 4 and 5, produces a large initial temperature gradient in these zones relative to the others (solid colour lines in Figure 5). The second is that the highest temperature zones at equilibrium are 3 and 4, and the

lowest temperature zones at equilibrium are 6 and 1. All zones approach an equilibrium temperature between 274.1°K and 282.3°K after a model year (Table 2). By reducing the inter-zonal transfer coefficient between zones 4 and 5 (dashed lines in Figure 5), we can alter the characteristics of a few zones dramatically. The most obvious of which are zones 4, 5, and, perhaps surprisingly, zone 6. These alterations include a reduction in the initial rate of change in temperature and will be analyzed further in Section 3.1.

2.2 Climate Model Following Single Volcanic Eruption

Figure 6 shows the effect of a single eruption on zonal temperatures initially at steady-state. The eruption occurs in zone 4 after 1 year, as indicated by the vertical dashed line. Zone 4 is immediately affected by the solar occlusion and shows a decrease in temperature. A time lag between the zonal temperature responses is clearly visible with zones at a greater distance from zone 4 showing a larger time lag. The recovery of each zone to its equilibrium temperature occurs over approximately 15 years after the eruption. The equilibrium temperature values are the same post-eruption as they are pre-eruption.

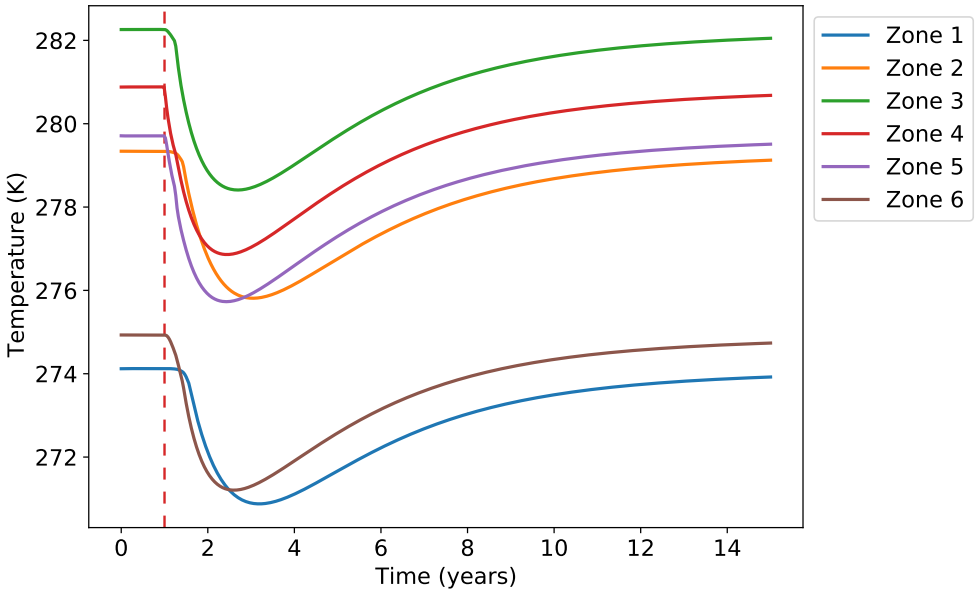

Figure 6: Reduction in solar forcing post eruption results in temperature drop.

2.3 Stochastic Volcanic Eruptions

Figure 7 shows a model result that includes multiple eruptions following the Poisson process defined in section 1.2.3. Vertical dashed lines represent an eruption with a coloured by the zone the eruption occurred. The eruption intensity parameters used are given in table 3

Zone	$\lambda_k[\text{yr}^{-1}]$
1	100
2	50
3	20
4	20
5	50
6	100

Table 3: Volcanic intensity rate parameters

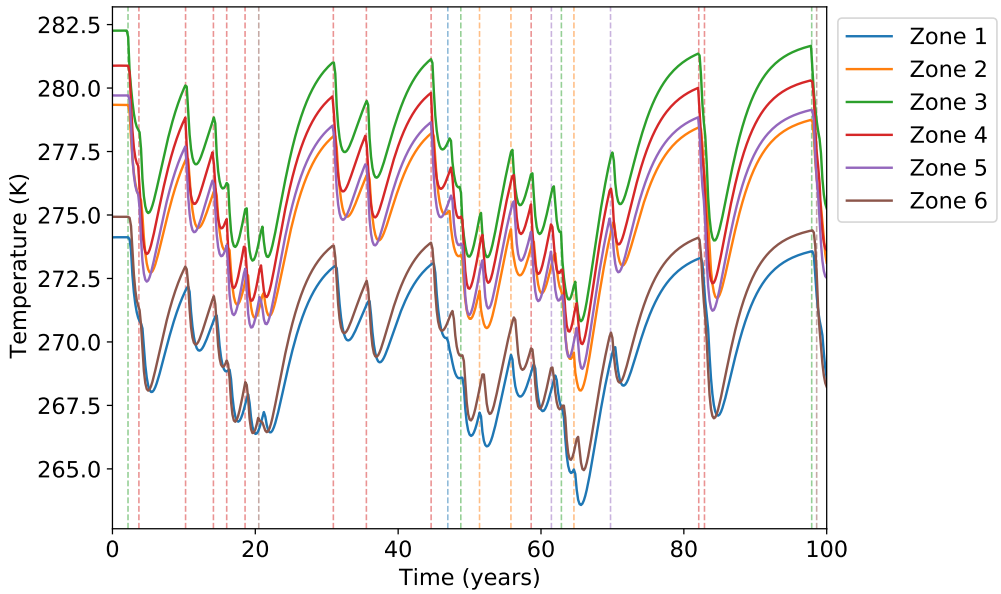

Figure 7: Stochastic eruption distribution following Poisson distribution. Vertical dotted lines are colored based on the zone the eruption occurred in, and their placement is the point in time at which the eruption is initiated.

The model was run for 100 years to show multiple cycles of temperature drops and recoveries. From Figure 7, we see that following each eruption is a decline in zonal temperatures, and sufficiently close eruptions, in time, compound that effect. The distribution lag associated with aerosol spreading is still represented numerically, though a lag of a few months is difficult to discern visually on this extended time scale.

2.4 The Ice-Albedo Effect

Figure 8 shows the result of the temperature dependent albedo from in equation 4 coupled with our climate model in equation 1. The temperature ranges for the nonlinear albedo model are coloured similar to figure 4. We recognize three temperature equilibria, two of which are stable and one that is unstable. The equilibrium temperature distributions are shown in table 4.

Zone	Warm Earth Equilibrium Temperature [K]	Unstable Equilibrium Temperature [K]	Snowball Earth Equilibrium Temperature [K]
1	274.02	251.08	231.91
2	279.27	255.03	234.30
3	282.21	258.31	236.23
4	280.83	257.78	236.13
5	279.66	256.98	235.70
6	274.83	253.11	233.20

Table 4: Ice-albedo effect equilibrium temperature distributions

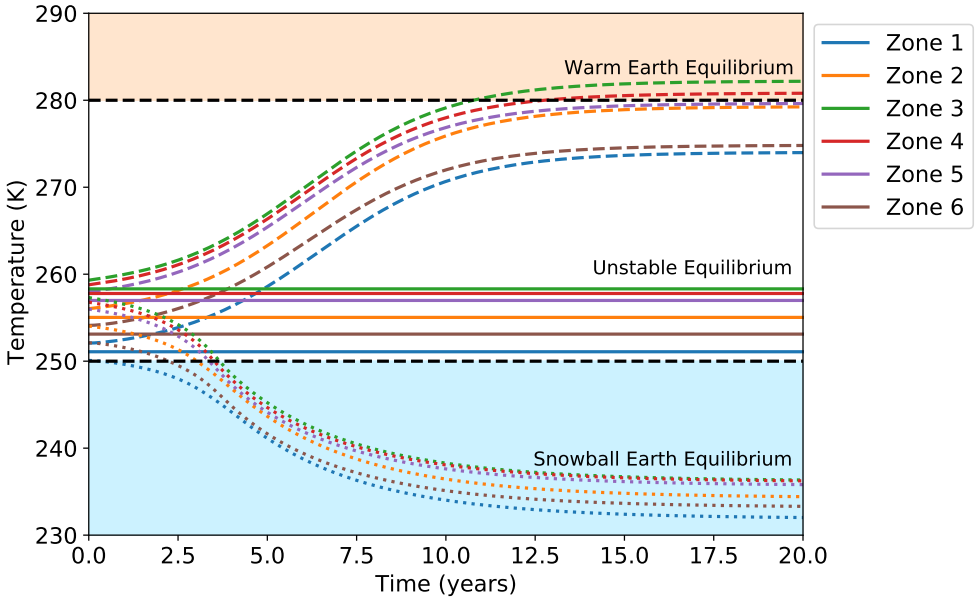

Figure 8: Integrating through climate model incorporating both stochastic volcanic eruptions and ice-albedo feedback parameterization.

A model started with an initial temperature distribution at the unstable equilibrium (solid lines in figure 8) remains at the unstable equilibrium.

A model started with an initial temperature distribution perturbed slightly above the unstable equilibrium (dashed lines in figure 8) asymptotically approaches the "warm Earth" equilibrium given in table 4.

A model started with an initial temperature distribution perturbed slightly below the unstable equilibrium (dotted lines in figure 8) asymptotically approaches the "snowball Earth" equilibrium given in table 4. The temperature difference between high-latitudinal and mid-latitudinal zones is much smaller for the snowball Earth equilibrium compared to the warm Earth equilibrium.

Zone	Stable Eruption Frequency $\lambda_k[\mathrm{yr}^{-1}]$	Unstable Eruption Frequency $\lambda_k[\mathrm{yr}^{-1}]$
1	150	100
2	75	50
3	50	20
4	50	20
5	75	50
6	150	100

Table 5: Volcanic intensity rate parameters for the volcanism with ice-albedo feedback models

2.5 Fire and Ice: Stochastic Volcanism and the Ice-Albedo Feedback

Figure 9 shows the results of two models that combine volcanism defined in section 1.2 with the ice-albedo feedback defined in section 1.3. The temperature ranges for the nonlinear albedo model are coloured similar to figure 4. The "Stable Eruption Frequency" and "Unstable Eruption Frequency" models were forced with the eruption intensity rate parameters shown in table 5.

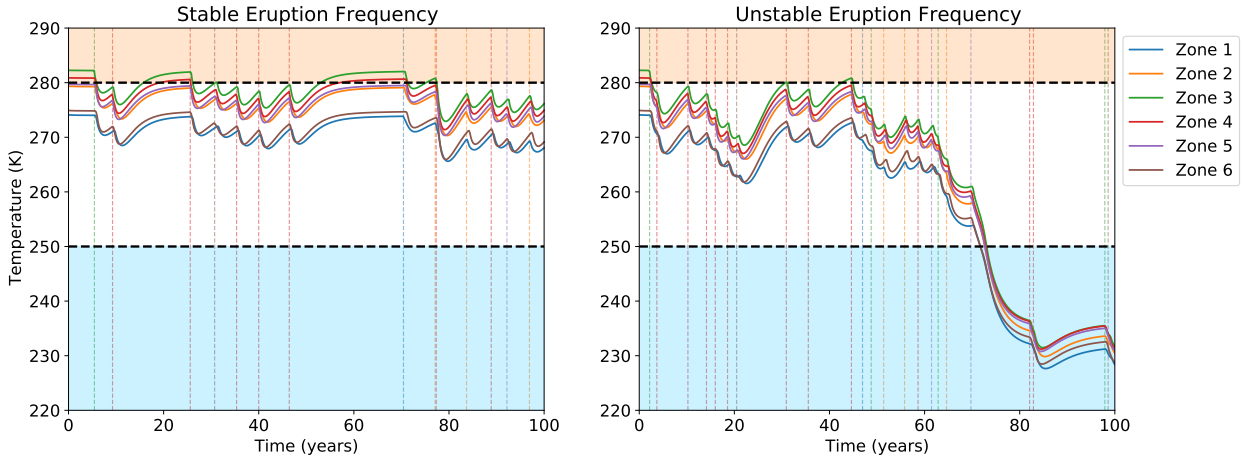

Figure 9: Model results for volcanism combined with the ice-albedo feedback.

The stable eruption frequency model oscillates around the warm Earth equilibrium shown in section 2.4. The unstable eruption frequency oscillates around the warm Earth equilibrium for approximately 70 years before it quickly drops to oscillate around the snowball Earth equilibrium.

3 Discussion

Here we will discuss the possible processes behind the numerical behavior of our Figures in Section 2 in order to elucidate the connection between our mathematical and computational results with their underlying physics.

3.1 Steady-State Climate Model: No Volcanism

Zones 4 and 5 experience a large initial temperature gradient due to a heat transfer coefficient indicative of Gulf Stream circulation processes that is larger than the transfer coefficients between other zones (Figure 5). This causes zones 4 and 5 to approach their equilibrium values more quickly. For example, zone 5 reaches its approximate equilibrium temperature within the first two months of the model year because the efficiency of heat transfer between these zones is greater than between others.

Zones 3 and 4 are the warmest zones due to their proximity to Earth's equator. Both lie within 30°N/S of the equator, and hence have the largest effective surface area, coupled with a low albedo due to a high land and sea fraction versus ice fraction (See Table 9). This increases these zones' retention of incoming solar radiative heating by reducing the amount lost to space as out-going, long-wave radiation (OLR). Zone 3 may be hotter than zone 4 due to smaller transfer coefficients between its adjacent zones than compared with zone 4, where heat transfer occurs rapidly due to influence from the Gulf Stream across the boundary of zone 4 and 5.

Conversely, zones 1 and 6 are the coldest zones at equilibrium due to their placement at Earth's high latitudes (> 60°N/S). This reduces their effective surface area such that less total solar insolation occurs, alongside a higher albedo due to a dominating ice fraction. This causes the OLR to be larger relative to incoming radiative heating than in the case of the other zones. Hence, temperature at equilibrium in zones 1 and 6 is lower. Zone 1 may be colder than zone 6 due to a higher albedo associated with a marginally larger ice fraction that increases OLR even relative to zone 6.

Comparing the solid and dashed lines in Figure 5, there is a general trend of reduced rate of change in temperature for several northern latitudinal zones. Zones 4 and 5 experience the greatest deviation from the original approach to equilibrium as this change is at their boundary of separation and directly reduces the amount of heat exchange between them. Zone 6 also experiences a reduction in the rate of approach to equilibrium due to its nonlinear relation with zone 5. As we can see, these effects are compounded in zones closest to zones 4 and 5, such that at sufficient separation, approaches to equilibrium are not noticeably affected. This is evident in zones 2 and 1, and suggests they have little dependence on temperature characteristics within the northern zones.

3.2 Volcanic Eruptions

One of the aims of our study was to investigate the short-term impact of volcanism on Earth's climate. The occlusion factor introduced in section 1.2.1 ultimately acts to cool the climate by blocking direct solar radiation from reaching the Earth's surface.

An interesting result is the difference in time scales for the occluding effect of an eruption and the subsequent recovery time of the climate. Figure 2 shows that suspended aerosols block less than 5% of direct solar radiation 2 years after an eruption. On the other hand,

figure 6 shows that it takes over a decade before the climate recovers to within 5% of its equilibrium temperature. This demonstrates that the climate feels the effects of volcanic aerosol occlusion even after the aerosols have dissipated and no longer block solar radiation.

The longer recovery time increases the susceptivity of the climate to compounding temperature drops from multiple eruptions, as see in figure 7. Temperatures are forced to values over 10 degrees below their equilibrium values during intense volcanic episodes. As we will see, these high intensity volcanic episodes can be a trigger that drives to Earth away from its initial equilibrium into a snowball Earth state.

3.3 The Ice-Albedo Effect

The nonlinear albedo dependence on temperature defined in equation 4 ultimately gives rise to three equilibrium conditions, as illustrated in figure 8. The "warm Earth" equilibrium represents conditions where the ice-albedo feedback has a small effect on the Earth's global energy balance. A small decrease in temperature near this equilibrium is compensated by an increase in heat flow from adjacent zones as well as a net positive flux of radiative energy from the sun which acts to increase the temperature. Even when temperatures fall in the variable albedo temperature range (i.e. $250\text{K} < T < 280\text{K}$), no ice-albedo runaway is observed. There is a slight decrease in equilibrium temperatures for the warm Earth equilibrium when compared to the equilibrium for the model with no ice-albedo feedback (2 and 4) due to some of the equilibrium temperatures falling in the variable albedo range.

3.4 Fire and Ice: Stochastic Volcanism and the Ice-Albedo Feedback

4 Conclusion

We saw that: In that case, under what conditions could Earth recover form the snowball solution? This model only investigates the effects of SO2 on the energy balance, not considering the influence of CO2. CO2 is a greenhouse gas, meaning that it efficiently absorbs the incoming solar radiation Volcanic eruptions

4.1 Future Work

5 Ancillary Information

5.1 Author Contributions

Section	Subsection	Contributors
Graphic	Box-Model	M
Code	Steady-State Climate	P and E
Code	Perturbation: Single Volcanic Eruption	P, E, and M
Code	Snowball Earth	P, E, and M
Introduction		M
Results	Steady-State Climate	n/a
Results	Perturbation: Single Volcanic Eruption	n/a
Results	Snowball Earth	n/a
Discussion	Steady-State Climate Model	n/a
Discussion	Perturbation: Single Volcanic Eruption	n/a
Discussion	Snowball Earth	n/a
Conclusion	Future Work	n/a
Conclusion	Summary	n/a

Table 6: In descending order: names depict relative contribution to sections with more than one contributor.

5.2 Algorithm Development

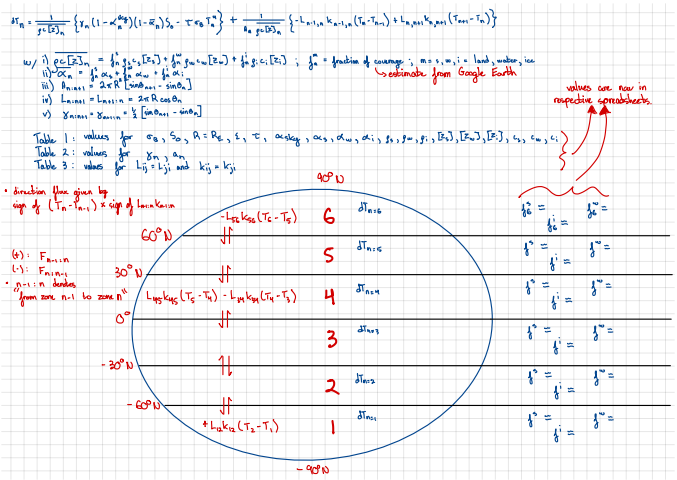

Figure 10: Sketch depicting zone intervals and necessary parameters for numerical solving.

1. Identify 6 latitudinal zones. Namely between $0-30°NS$, $30-60°NS$ and $60-90°NS$.

2. Determine parameters associated with each area.

3. Solve ODE numerically using Paul Matlashewski's ClimateModel.py library.

5.3 Data

5.3.1 Eruption Times Series

Table 7: Eruption Times Series 1

date	value
1982.396551724138	347.0380363253488
1982.4827586206898	369.1787312450645
1982.5689655172414	384.4491971571466
1982.683908045977	407.35434763534266
1982.8275862068965	439.42090023690446
1983	479.12213740458014
1983.603448275862	488.3054751250329
1983.9195402298851	499.7679213828201
1984.6379310344828	506.6655698868123
1985.6149425287356	518.9166008598754
1986.3620689655172	521.2351934719663
1987.1666666666667	526.6094147582697
1988	526.6412213740458
1988.7183908045977	527.4319996490304
1990.3850574712644	525.9688953233307
1991.0747126436781	529.8120119329649

Table 8: Eruption Time Series 2

date	value
1991.6781609195402	390.1403878213565
1991.8793103448277	412.28546986048957
1992.1954022988507	439.7784504694218
1992.4540229885058	464.21580240414147
1993.1436781609195	502.4100640519435
1993.8333333333335	516.940203562341
1994.6954022988507	523.843335965605
1995.7298850574714	527.6996139334913
1996.9655172413793	530.800210581732
1998.057471264368	532.3686057734492
1998.4597701149426	531.6206019127841

5.3.2 Parameters

Table 9: Zonal Parameters

	Parameter	Value
Zone 1	Geometric Factor, γ_1	0.1076
	Area Fraction, A_1	0.067
	Land Fraction, f_1^s	0.0
	Ocean Fraction, f_1^w	0.550925926
	Ice Fraction, f_1^i	0.449074074
Zone 2	Geometric Factor, γ_2	0.2277
	Area Fraction, A_2	0.183
	Land Fraction, f_2^s	0.074074074
	Ocean Fraction, f_2^w	0.925925926
	Ice Fraction, f_2^i	0.0
Zone 3	Geometric Factor, γ_3	0.3045
	Area Fraction, A_3	0.25
	Land Fraction, f_3^s	0.240740741
	Ocean Fraction, f_3^w	0.759259259
	Ice Fraction, f_3^i	0.0
Zone 4	Geometric Factor, γ_4	0.3045
	Area Fraction, A_4	0.25
	Land Fraction, f_4^s	0.3101851851
	Ocean Fraction, f_4^w	0.689814815
	Ice Fraction, f_4^i	0.0
Zone 5	Geometric Factor, γ_5	0.2277
	Area Fraction, A_5	0.183
	Land Fraction, f_5^s	0.694444444
	Ocean Fraction, f_5^w	0.305555556
	Ice Fraction, f_5^i	0.0
Zone 6	Geometric Factor, γ_6	0.1076
	Area Fraction, A_6	0.067
	Land Fraction, f_6^s	0.277777778
	Ocean Fraction, f_6^w	0.652777778
	Ice Fraction, f_6^i	0.069444444

Table 10: Global Parameters

Parameter	Value	Units
Stefan-Boltzmann Constant, σ_B	5.6696e-8	$Wm^{-2}K^{-4}$
Solar Constant, S_0	1368	Wm^{-2}
Earth Radius, R_E	6371e3	m
Earth Total Emissivity, ϵ	1	
Surfacea Area of Earth, A_E	πR_E^2	m^2
Atmospheric Transmissivity, τ	0.63	
Atmospheric Albedo, α_{sky}	0.2	
Land Albedo, α_s	0.4	
Ocean Albedo, α_w	0.1	
Ice Albedo, α_i	0.6	
Land Density, ρ_s	2500	kgm^{-3}
Ocean Density, ρ_w	1028	kgm^{-3}
Ice Density, ρ_i	900	kgm^{-3}
Land Thermal Scale Depth, $[Z_s]$	1.0	m
Ocean Thermal Scale Depth, $[Z_w]$	70.0	m
Ice Thermal Scale Depth, $[Z_i]$	1.0	m
Land Specific Heat Capacity, c_s	790	$JkgK^{-1}$
Ocean Specific Heat Capacity, c_w	4187	$JkgK^{-1}$
Ice Specific Heat Capacity, c_i	2060	$JkgK^{-1}$

6 References

References

Budyko, M. (Dec. 1969). "The effect of solar radiation variations on the climate of Earth". In: *Tellus* 21, 5, pp. 611–619. URL: https://doi.org/10.3402/tellusa.v21i5.10109.

Robock, A. (May 2000). "Volcanic eruptions and climate". In: *Reviews of Geophysics* 38, 2, pp. 191–219.